Chapter 10

Theoretical Studies of Titanium Dioxide for Dye-Sensitized Solar Cell and Photocatalytic Reaction

Fu-Quan Bai, Wei Li and Hong-Xing Zhang

Additional information is available at the end of the chapter

http://dx.doi.org/10.5772/intechopen.68745

Abstract

This chapter aims to provide researchers in the field of photovoltaics with the valuable information and knowledge needed to understand the physics and modeling of titanium dioxide for dye-sensitized solar cell and photocatalytic reaction. The electronic band structure of titanium dioxide, the treatment of the excited state of titanium dioxide, the molecular dynamics and ultrafast quantum dynamics simulations, and several promising photocatalytic schemes and important considerations for theoretical study are addressed and reviewed. The advanced computational strategies and methods and optimized models to achieve exact simulation are described and discussed, including first principle calculations, nonadiabatic molecular and quantum dynamics, wave function propagation methods, and surface construction of titanium dioxide. These advanced theoretical investigations have become highly active areas of photovoltaics research and powerful tools for the supplement and prediction of related experimental efforts.

Keywords: electronic band structure, first principle calculation, excited state, molecular modeling, photophysical process, photochemistry and photocatalysis

1. Introduction

With the increasing concerns about energy issues and the associated environmental pollution, renewable energy technologies are devoted to being the most promising strategy for sustainable energy supply [1, 2]. Among all of these technologies, including hydro, solar, wind, geothermal heat, and biomass, photovoltaic (PV) technology that converts solar energy into electricity have attracted considerable attention. At present, the solid-state junction devices based on silicon material have dominated PV solar energy converters. However, the light-induced degradation of silicon materials limits the device stability and hinders its effective. Third-generation photovoltaics are

able to produce high-efficiency photon to electricity conversion devices at a cheaper production cost. This is a consensus that the price is decreased, and the cell efficiency is maintained for the third-generation solar cell. There are unique features for this kind of cells; the cell should be sensitized by a photoactive material among dye, quantum dots (QDs), and perovskite system [3]. Work on sensitized photovoltaics started during the 1970s with the use of organic dyes as the sensitizer [4]. The similar structure of these solar cells is that in the case of the original design: The cell has three primary parts, glass sheet with transparent conducting oxide coating (ITO or FTO) as anode and the counter electrode (CE) on top and bottom, respectively; and TiO_2 film deposits on the conductive side of the glass sheet which is then immersed in a mixture of a photosensitizer and a solvent for charge transport. The working principle looks also dynamically analogical. But in quantum dot-sensitized solar cells (QDSSCs), that replaced organic dyes in dye-sensitized solar cells (DSSCs) with inorganic sensitizers, the total performance is promoted by the utilization of nano-sized crystals with a short band gap and a high extinction coefficient. Along with this line of thought, since 2009, the perovskite materials as sensitizers have been used initially and works very well with the solid-state hole transfer material. Until now, its efficiency has touched over 21% [5, 6]. For DSSCs, the photoanode components are the dye sensitizer, a mesoporous semiconducting oxide layer and a transparent conducting oxide (TCO). In DSSCs, the transport of charges (electrons) to the external circuit begins when electrons exit the semiconducting network layer and ends when the redox mediator in the charge transport medium returns them to the sensitizers [7]. The photoelectric anode consists of a TCO substrate with a semiconductor oxide layer (usually TiO_2) and a dye sensitizer. In fact, there are two TiO_2 layers. The first layer is a slender and blocking layer to inhibit electron recombination with ionized dyes and/or mediators. The second layer is more than 20–30 nm thickness of mesoporous TiO_2. The larger surface area of the mesoporous TiO_2 area allows a greater amount of dye to be adsorbed on its surface. An electrolyte usually with an iodide/triiodide couple is needed for DSSC. The electrolyte can be in liquid/gel or solid form.

2. The electronic band structure of titanium dioxide

A typical DSSC consists of the wide band gap TiO_2 semiconductor, the dye is employed to absorb light radiation, and the photo-excited electrons are subsequently transferred to the TiO_2 [8]. The fast interfacial electron transfer between the dye and TiO_2 could, in principle, minimize the loss of the utilized photon energy as heat through the electron-phonon relaxation pathway. Through this process, the absorption range can be efficiently extended to the visible region, which dominates the solar spectrum. In the many semiconductor metal oxides, titanium dioxide (TiO_2) is expected to play an import role in PV devices due to its high chemical and optical stability, nontoxicity, and corrosion resistance, low-cost [9]. TiO_2 is a semiconductor material with a band gap of ~3.2 eV, corresponding to a wavelength of ~390 nm. The anatase structure is preferred over other polymorphs for solar cell applications because of its potentially higher conduction band edge energy and lower recombination rate of electron–hole pairs [10]. This is not the case for excellent UV photocatalysts such as rutile or anatase polymorphs of TiO_2 due to the rather high band gap that these materials exhibit (**Figure 1**). This has prompted chemists and material scientists to search for modifications of

http://dx.doi.org/10.5772/intechopen.68745

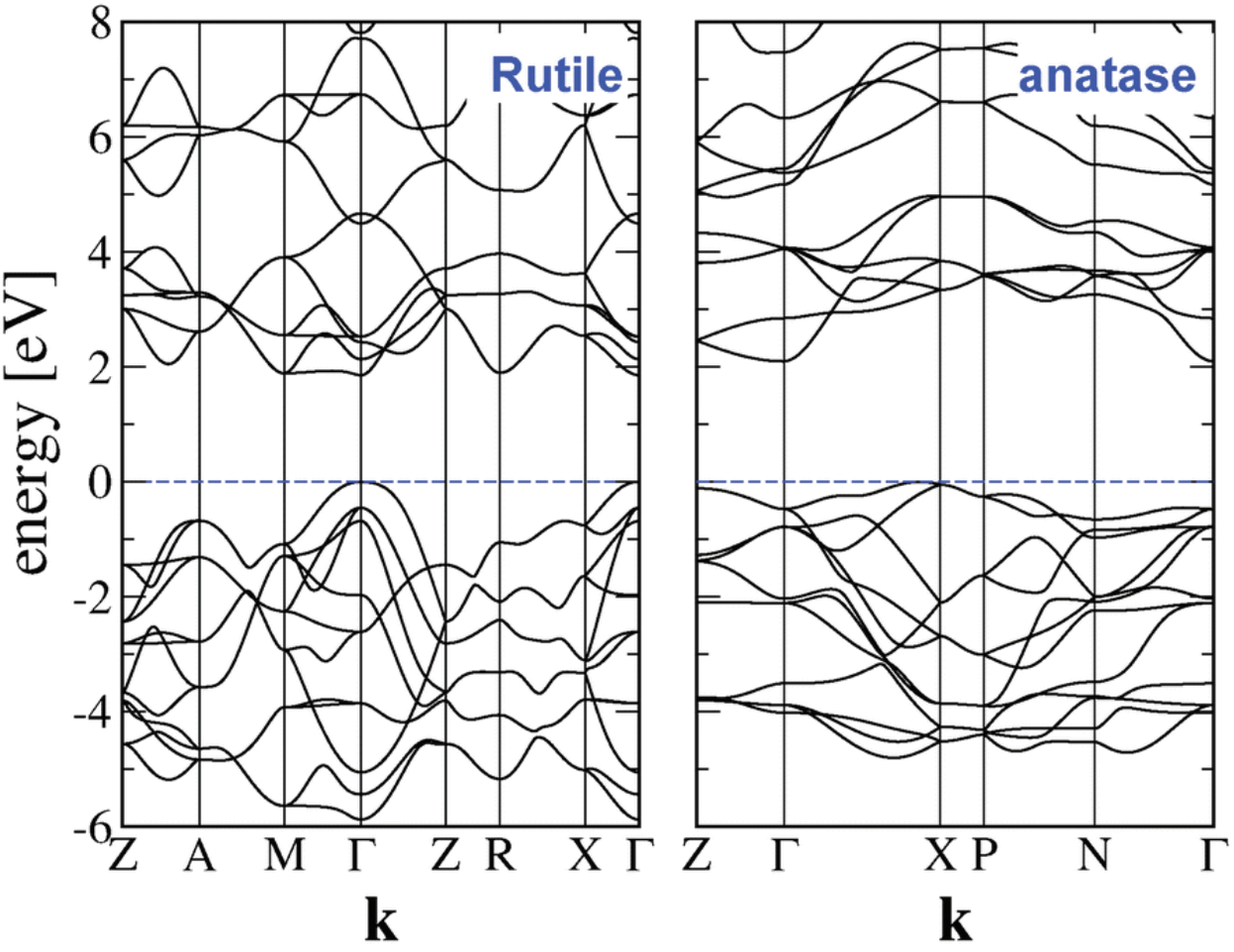

Figure 1. Band structure of rutile and anatase calculated by PBEsol with the respectively relaxed crystal structures. (Copyright 2016 Royal Society of Chemistry).

TiO_2 which could exhibit photocatalytic activity under visible light. Doping seemed to be one of the obvious options.

3. First principle calculations and modeling simulation

In this section, we will provide a comprehensive insight on the different levels of theoretical methods used in the description of the electronic structures, and particularly attention was paid to methods involved in the excited state in the metal oxide. At present, the wave function-based ab initio method and density functional theory (DFT) are the two main types of theoretical method. However, both methods have drawbacks, which are Born-Oppenheimer (BO) approximation break down when treating the excited state potential energy surface (PES). Of course, the BO approximation is good for description of the ground state properties, such as the geometry optimization, electronic structure calculation, since the nuclei are fixed for the ground state. Stochastic methods need to be developed to properly account for the excited state, but this kind of method is usually time-consuming since it requires the evaluation of the second-derivative of

Hessian matrix. In this respect, choosing a particular computational method must take a compromise between accuracy and its feasibility.

3.1. The DFT theory

Quantum mechanics calculations have widely used to address the physical and chemical properties of metal oxide. The level of the theoretical method includes Hartree-Fock (HF) self-consistent field (SCF), second-order Møller-Plesset (MP2) perturbation theory, coupled cluster (CC) theory, as well as the most popular DFT method. DFT has been the standard "answer" for the electronic structure calculations of a series of material systems, from molecules to solids, and from clusters to periodic systems. The one-electron density matrices can be expressed as follows:

$$\rho_0(\vec{X}) = N\int \Psi_0^*(\vec{X_1}, \vec{X_2}, \ldots, \vec{X_N})\Psi(\vec{X_1}, \vec{X_2}, \ldots, \vec{X_N})d_{\vec{X_2}}\ldots d_{\vec{X_N}} \quad (1)$$

where the subindex zero indicates density originates from the ground state wave function. For one N-electron system, DFT approximates the ground state energy of the system as a function of the electron density, that is to say, the ground state energy can be determined as long as the density function is given. However, the exact expression of density functional is still unknown. There are substantial works devoted to exploring the accurate density functionals. Generally, the density functional is given by:

$$E[\rho] = T_s[\rho] + V_{ert}[r] + V_{Coulomb}[\rho] + V_{XC}[\rho] \quad (2)$$

$T_s[\rho]$ is the kinetic energy term of the noninteracting electrons, the $V_{ert}[r]$ is the external potential, and $V_{Coulomb}$ represents the Coulomb repulsion. The last term $V_{XC}[\rho]$ accounts for the exchange-correlation effect, which is difficult to get the exact expression. The success of DFT depends on whether we can find out the appropriate approximations to the exchange-correlation term. Generalized gradient approximation (GGA) and local density approximation (LDA) are mostly used for exchange-correlation functionals in condensed matter systems, and meta-GGA and hybrid functionals are often used in isolated molecule. DFT in the local density approximation (LDA) and various GGA consistently predicts that anatase is more stable than rutile [11], and no significant improvement can be achieved when using more sophisticated DFT approaches, including hybrid functionals (PBE0 and HSE06) [12] and DFT plus the Hubbard U correction (DFT + U) [13, 14], and various dispersion-corrected DFT methods. A similar situation also occurs for the DFT + U method, which predicts rutile to be more stable only if an unphysically large U value is used.

3.2. The treatment of excited state of titanium dioxide

The relative stability of different polymorphic phases of a material is often addressed in terms of the ground state total energy [15, 16], but generally speaking, other degrees of freedom, including, in particular, those of nuclei vibration, may also play a significant role. The contributions of vibration, including the zero-point energy (ZPE) and finite-temperature

http://dx.doi.org/10.5772/intechopen.68745

vibration enthalpy and entropy, can be obtained from the phonon spectrum calculated in the harmonic approximation. We have found the resort that by considering high-order correlations in the adiabatic connection fluctuation–dissipation theory with the random phase approximation (ACFDT-RPA), rutile is correctly predicted to be more stable than anatase, which can be physically attributed to different characters in the electronic band structure of rutile and anatase, including, in particular, that rutile has a smaller band gap than anatase [17]. In the framework of DFT, the most efficient way to approach the excitation problem is its time-dependent formalism (TD-DFT) based on the Runge-Gross theorems, which may be seen as a consequence of the time-dependent Schrödinger equation (TD-SE) to describe the time-dependent phenomena [18]. TD-DFT can be viewed an alternative formulation of time-dependent quantum mechanics but, in contrast to the normal approach that relies on wave functions and on the many-body Schrödinger equation, its basic variable is the one-body electron density. The key exceptions so far that should be mentioned here are the development of extending CIS, TDHF, and TD-DFT to one-dimensional system like a one-dimensional chain of hydrogen molecules by Hirata et al. [19, 20], and the recent implementation of TD-DFT to periodic systems in the CRYSTAL code by Bernasconi et al. [21]. Walker et al. also developed the Turbo TDDFT code to make it is possible to carry out TD-DFT calculations using plane wave basis sets for the large condensed system [22]. However, in spite of using periodic boundary conditions, which is a necessary requirement to date, this formalism is only implemented for finite systems. The introduction of a portion of the Fock exchange is not the only strategy to improve the description of the band gap in the oxide and related materials, where LDA and GGA are even qualitatively ineffective. One common method is to add two parameters to the LDA or GGA exchange-correlation function, as in the Hubbard model, an exchange (J) term between electrons with the same orbital angular momentum, to mimic the effective field Coulomb (U) term [23].

Among the various possible approaches going beyond the DFT band structure calculations to predict the band gap of oxides, a growing interest is nowadays dedicated to the so-called GW quasiparticle approach (Green's function G and the screened Coulomb interaction W). The quasiparticle approach permits simulation of the ejection or the absorption of an electron from an N-electron state to an $N \pm 1$ electron state. And then, the direct comparison of the calculated results with photoemission or inverse-photoemission experiments can be performed based on this in principle. The first formulation of the GW method dates back to the work from 1965. However, the approach was not applied to large-scale, numerical electronic structure calculations before the mid-eighties. The resulting band gaps compare much better with experiment. The GW approximation is an approximation made in order to calculate the self-energy of a many-body system of electrons. The approximation is the expansion of the self-energy in terms of the single particle Green's function G and the screened Coulomb interaction W [24]. The whole formalism is rather complex, and a more detailed description can be found in the review paper of Huang and Carter [25]. Nevertheless, the ever-growing computational facilities have made GW calculations indeed attractive in solid-state computational simulations. The GW approach consists of updating both Green's function and the dielectric potential at every iteration. The amplitudes and the excitation energies, E, can be obtained from the Bethe-Salpeter equation (BSE), which can be written as an eigenvalue equation according to

$$\left[\left(\varepsilon_p^{QP} - \varepsilon_h^{QP}\right) - E\right] c_{ph} + \sum_{p'h'} K_{ph,p'h'} c_{p'h'} = 0 \tag{3}$$

where ε_p^{QP} and ε_h^{QP} are the quasiparticle eigenvalues of the particle and the hole, respectively. The sum in Eq. (3) runs over the kernel $K_{ph,p'h'}$, which can be split into two terms:

$$\boldsymbol{K}_{ph,p'h'} = \boldsymbol{K}_{ph,p'h'}^{exc} + \boldsymbol{K}_{ph,p'h'}^{dir} \tag{4}$$

$\boldsymbol{K}_{ph,p'h'}^{exc}$ is the particle−hole exchange operator, which has the usual form:

$$\boldsymbol{K}_{ph,p'h'}^{exc} = \int dx dx' \Psi_p^*(x) \Psi_h(x) \frac{1}{|x - x'|} \Psi_{p'}(x) \Psi_{h'}^*(x') \tag{5}$$

$\boldsymbol{K}_{ph,p'h'}^{dir}$ is the screened Coulomb operator, where a term depending on the inverse screened dielectric tensor is applied, similarly to the case for GW:

$$\boldsymbol{K}_{ph,p'h'}^{dir} = \int dx dx' \Psi_p^*(x) \Psi_h(x') \eta^{-1}(x, x') \frac{1}{|x - x'|} \Psi_{p'}(x) \Psi_{h'}^*(x') \tag{6}$$

In the same framework, neutral excitations (e.g., optical and energy-loss spectra) are also well described today through the solution of the Bethe-Salpeter equation. A self-contained method is able to perform both the starting self-consistent field calculation in the generalized Kohn-Sham (gKS) framework and the many-body perturbation theory (MBPT) post-treatment, and then that can produce GW quasiparticle energies, optical spectra and the dielectric screening, prior to Eqs. (3)–(6) through a solution of the BSE. Entertainingly, Onida et al. have shown that the BSE is intimately related to the linear response formulation of TDDFT [26].

3.3. The molecular dynamics simulation

The extremely small size of these particles makes them ideal candidates for investigation with molecular dynamics (MD) simulation, which has been a long-established simulation technique to extensively investigate structural and dynamic properties of solids and fluids at the atomic scale. A large number of force fields have been reported in the literature for modeling TiO_2 polymorphs [27–29]. For example, based on the Hubbard-corrected DFT + U and first-principles molecular dynamics (FPMD) simulations, facet-dependent trapping and dynamics of excess electrons at anatase TiO_2 surfaces and aqueous interfaces could be achieved. Whereas no electron trapping is observed on the (101) surface in vacuo, an excess electron at the aqueous (101) interface can trigger water dissociation and become trapped into a stable surface Ti^{3+}-bridging OH complex [30].

4. The titanium dioxide used in DSSC

TiO_2 semiconductor is the widely used electron conductor in Grätzel-type photovoltaic DSSC, because of its low-cost and ease of synthesis. A typical DSSC consists of the wide band gap

http://dx.doi.org/10.5772/intechopen.68745

TiO_2 semiconductor, the dye is employed to absorb light radiation, and the photo-excited electrons are subsequently transferred to the TiO_2. Two major crystal phases of TiO_2: rutile (a) and anatase (b), are shown in **Figure 2**. The rutile phase is energetically stable since the crystal structure is symmetric. Each Ti atom is sixfold, and coordinated with threefold O atom. The anatase phase has the similar coordination number as rutile but with asymmetrical structure. DFT calculation suggests that the anatase (101) surface is the most active surface since it has unpassivated Ti and O atoms, which has been widely used to simulate the interface electron transfer process [31, 32].

4.1. The rule of titanium dioxide

So far, solid-state devices based on silicon have dominated photovoltaic solar converters. However, light-induced degradation of silicon materials limits device stability, while the relatively high cost (high purity) of photovoltaic power generation hinders its effective competition with fossil energy. Pure silicon has a little use, but doped silicon is the basis for most semiconductors. An attractive alternative to crystalline silicon photovoltaic devices is a unit made of mesoscopic inorganic semiconductors that can be easily prepared and provide a very low-cost manufacturing prospect. In these devices, inorganic semiconductors are primarily used as electron acceptors and provide direct or tortuous paths for electron transport, and in some cases, they can act as scaffolds for absorbing light collectors. Holes reside in the valence band, a level below the conduction band. Doping with an electron acceptor, an atom which may accept an electron, creates a deficiency of electrons, the same as an excess of holes. Among many semiconductor metal oxides, TiO_2 nanomaterials appear to be differentiated candidates because of their high chemical and optical stability, non-toxic, low-cost and corrosion resistance. Anatase TiO_2 has a crystal structure corresponding to the tetragonal system, but the distortion of the TiO_6 octahedron is slightly larger for the anatase phase. The anatase structure with improved electrical properties is superior to other polymorphs used in solar cells because of its potentially higher conduction band edge energy, and it enables

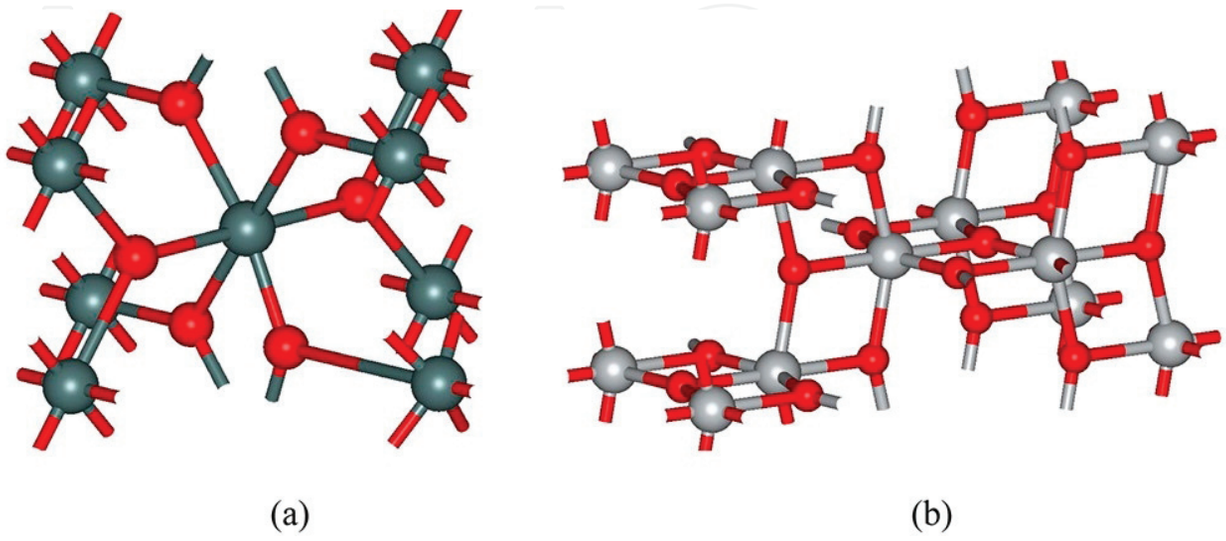

Figure 2. The crystal structure of rutile (a) and anatase (b) TiO_2. (Copyright 2013 American Chemistry Society).

remarkably efficient spatial separation of electron–hole pairs on the submicrosecond time scale. The physical and chemical properties of TiO_2 nanocrystals are affected not only by the intrinsic electronic structure but also by their size, shape, texture, doping and surface properties. The smaller effective mass in anatase is consistent with the high mobility, band like conduction observed in anatase crystals. It is also responsible for the very shallow donor energies in anatase. In addition to the large surface area, TiO_2 nanomaterials should also have high electron mobility, making it possible to efficiently collect electrons injected into TiO_2. Since the defects in the TiO_2 nanomaterials can be used as electron captures and present in the grain boundaries at the junctions between the nano-sized particles, it is expected to use a network structure consisting of TiO_2 monocrystalline nanowires rather than TiO_2 nanoparticles rapid electronic transmission. Besides, the properties of TiO_2 also strongly relay on the modifications of the TiO_2 material host and on the interactions of TiO_2 materials with the environment. The surface modification not only affects the interfacial energy offset but also has significant impact on the charge separation, transport, and recombination processes.

4.2. The charge transfer process and Marcus theory

The Marcus theory is the most fundamental theory for a description of the electron transfer (ET) process in condensed material. Its formula can be given by [33–35]:

$$k(T) = \kappa A\sigma^2 \exp\left\{-\frac{w^r + \frac{\lambda}{4}\left(1 + \frac{\Delta\tilde{G}^o}{\lambda}\right)^2}{k_B T}\right\} \tag{7}$$

$$\Delta\tilde{G}^o = \Delta G^o + w^p - w^r \tag{8}$$

The above equation explicitly takes various contributions to the free energy into account, where $A\sigma^2$represents the collision frequency, and σ is the distance between the reacting species. ΔG^o is the reaction free energy, $\Delta\tilde{G}^o$ is the free energy after work correction. w^r and w^p are the work corresponds to the reactant and product state. λ is the reorganization energy, contains the contributions coming from the reactant and solvent.

$$\lambda = \lambda_r + \lambda_{sol} \tag{9}$$

The reactant and solvent contributions of the reorganization energy are given by:

$$\lambda_r = \sum_i \frac{f_i^{(r)} f_i^{(p)}}{f_i^{(r)} + f_i^{(p)}} (\Delta q_i)^2 \tag{10}$$

$$\lambda_{sol} = (\Delta e)^2 \left(\frac{1}{2R_1} + \frac{1}{2R_2} - \frac{1}{\sigma}\right)\left(\frac{1}{\varepsilon_s} - \frac{1}{\varepsilon_{op}}\right) \tag{11}$$

http://dx.doi.org/10.5772/intechopen.68745

where $f_i^{(r)}$ and $f_i^{(p)}$ are the force constants of the given normal mode for reactant and product states, respectively; Δq is the changes of the ith nuclear coordinate; and Δe is the amount of transferred charge from reactant to product. ε_s and ε_{op} are dielectric constants of the solvent for static and optical. The original Marcus theory assumes that diabetic PES can correspond to the reactant and product states, and this simplifies the description of the ET.

4.3. The ultrafast quantum dynamics

Nonadiabatic ET involves the participation of the nuclear, the Fermi's Golden rule is usually employed to evaluate the electron transfer rate $K_{\mathrm{I->F}}$ of nonadiabatic ET.

$$k_{I\to F} = \frac{2\pi}{\hbar}|\langle F|H'|I\rangle|^2\delta(E_F - E_I) \tag{12}$$

This formula originates from the first-order time-dependent perturbation theory (TD-PT). Where $I\rangle$ is the initial state, $F\rangle$ is the final state, and H' is the time-dependent perturbation Hamiltonian due to the nuclei vibration. The advantage of FGR is that ET rate can be determined from electronic structure calculation, that is, the coupling between initial and final state depends on the atomic orbital coefficient. This greatly simplifies the calculation of electron transfer for the chromophore-semiconductor system.

A conceptually similar but rougher approach is proposed by May, in which the rate constant derivates to be:

$$k_{i\to\{f\}} = 2\overline{\Gamma} = \frac{2\pi}{\hbar^2}\overline{N}|\overline{V_e}|^2 \tag{13}$$

This equation is based on linear response approaches, in which $\overline{\Gamma}$ is the absorption line broadening. $\overline{V_e}$ is average density of states. Labat and coworkers derivate an even more simple expression for the electron transfer time based on the Newns−Anderson approach [36]:

$$\tau = \frac{658}{\Delta} \tag{14}$$

Δ is the broadening of the dye donor orbital. Generally, this method gives the electron transfer timescale half of the experimental value [37].

The electron transfer rate constant estimated using Marcus and Fermi's golden rule can be calculated at different levels of theory method. But these methods just focus on the description of the single process. However, the electron transfer process might be subject to the influence of environment. Accurate estimation of the electron transfer rate depends on the exact solution of TD-SE, especially the nuclei part at the quantum mechanics level.

$$i\hbar\frac{\partial\tilde{\chi}_i\left(t, R(t)\right)}{\partial t} = \sum_j\left\{\left(T_{nucl} + E_j(R)\right)\delta_{ij} - \hbar^2\frac{d_{ij}^{(2)}}{2M}\right\}\tilde{\chi}_j(t, R(t)) \tag{15}$$

It is challenging to treat nuclei quantum mechanics. This is because a given system can contain a nucleus with different mass and speed. Therefore, it is difficult to developing a universe density functional to treat nuclei vibration. The accurate solution of Eq. (15) only fed with the small system based on the grid method. But as the size of the system increases, the above method becomes impractical. The alternative is to treat the nuclei classically, and then a semi-classical expression can be obtained:

$$i\hbar \frac{\partial \tilde{\chi}_i\left(t, R(t)\right)}{\partial t} = \sum_j \left\{ E_j(R)\delta_{ij} - i\hbar^2 \frac{p}{M} d_{ij}^{(1)} \right\} \tilde{\chi}_j\left(t, R(t)\right) \tag{16}$$

In the above equation, the classical momenta p is introduced. Surface hopping method is suitable for mimic the wave-packets branching using a classical trajectory. Fewest switches surface hopping (FSSH) is the most popular semi-classical method for nonadiabatic molecular dynamics. The electron transition rate from state *i* to state *j* at the small time interval $g(t)$ can be expressed as follows:

$$g_{i\to j}(t) = \max(0, P_{i\to j}(t)) \tag{17}$$

where

$$P_{i\to j}(t) = 2\frac{\int_t^{t+\Delta t} \mathrm{Re}\left(c_i^*(t') c_j(t') \frac{\vec{P}}{M} \vec{d}_{ij}(t') \right) dt'}{c_i^*(t) c_i(t)} \approx 2\frac{\mathrm{Re}\left(c_i^*(t) c_j(t) \frac{\vec{P}}{M} \vec{d}_{ij}(t') \right) \Delta t}{c_i^*(t) c_j(t)} \tag{18}$$

Here, $c_i(t)$ is the time-dependent expansion coefficient. The hopping probability is compared with a random number to determine whether it is hopped to a new state or remain in the current state. Nuclear velocity is rescaled to conserve the total energy. More details of the implementation of FSSH can be found in the literature [38, 39]. It is worthy of noting that classical path approximation (CPA) is employed for treating the large system. CPA assumes that the electron depends on nuclei motion, but a nucleus is independent of the electron, and this is the so-called quantum backreaction problem. CPA is valid in case the heavy nuclei has the large energy than a lighter electron, and this could enable the nuclear evolution is not affected by the electron-nuclear interaction. The use of CPA could lead to the large computational saving since the many stochastic surface hops can be achieved along the precomputed MD trajectory.

The original FSSH formulas take the hop-rejection into consideration, and this is given by the following:

$$g_{i\to j}(t) \to g_{i\to j}(t) b_{i\to j}(t) \tag{19}$$

$$b_{i\to j}(t) = \begin{cases} \exp\left(-\frac{E_j - E_i}{k_B T} \right), E_j > E_i \\ 1, E_j \le E_i \end{cases} \tag{20}$$

The transition probabilities $g_{i\to j}(t)$ in the above equation are rescaled by the Boltzmann factor, taking the detailed balance between transition up and transition down in energy.

http://dx.doi.org/10.5772/intechopen.68745

4.4. Wavefunction propagation methods

The previous section discussed the semi-classical method for nonadiabatic molecular dynamics. That semi-classical method does treat the nuclear classically. However, in some cases, the nuclear quantum effect cannot be neglected, for example, the evaluation of Franck-Condon factor involved in the electron excitation. Explicitly propagation of the nuclear wave function can achieve this goal. Methods like multiconfiguration time-dependent Hartree (MCTDH) method and quantized Hamiltonian dynamics (QHD) are developed for a different level of accuracy. These methods are based on the propagation of Gaussian wavepacket, which has been proposed to study the quantum effects of nuclear dynamics. The MCTDH method is one of the most accurate methods for wave-packet propagation. The nuclei wave function is expressed as follows:

$$\begin{aligned} &|\tilde{\chi}_i(t, R_1, R_2, \ldots R_f)\rangle \\ &= \sum_{j_1}^{n_1} \ldots \sum_{jf}^{n_f} A^1_{j_1 \ldots jf}(t) |\chi^1_{j_1}(t, R_1)\rangle \ldots |\chi^1_{j_f}(t, R_f)\rangle \end{aligned} \tag{21}$$

MCDTH provides the exact and accurate solution to the quantum description of nuclear behaviors. Therefore, it is extremely time-demanding in computation. Its complexity scales as N^f, where $f$is the number of freedom of the total system, while N^f is the number of the atomic orbital basis function. However, this method is only suitable for the system with limited atoms and has been improved using multilayer MCTDH (ML-MCTDH) technique:

$$|\tilde{\chi}_i(t, R_1, R_2, \ldots R_f)\rangle = \sum_{j_1}^{n_1} \ldots \sum_{j_p}^{n_p} A^1_{j_1 \ldots j_p}(t) |\chi^1_{j_1}(t, R_1^{coll,1})\rangle \ldots |\chi^1_{j_p}(t, R_p^{coll,1})\rangle \tag{22}$$

The concept of collective coordinates (*R*c°ll) is introduced. In principle, ML-MCTDH theory can be fed with the system contains several thousands of degrees of freedom [33].

In addition to the MCTDH method, quantum dynamics method based on the propagation of electron wave function is also of interest. Time-dependent electron wave function can be expressed as linear combination of atomic orbitals

$$|\varnothing(t)\rangle == \sum\nolimits_{i,\alpha} B_{i,\alpha}(t) |i, \alpha\rangle \tag{23}$$

$|i, \alpha\rangle$ is the corresponding atomic orbital α of atom i. The expansion coefficient can be expressed as follows:

$$B_{i,\alpha}(t) = \sum\nolimits_q Q^q_{i,\alpha} C_q \exp\left(-\frac{i}{\hbar} E_q t\right) \tag{24}$$

Solving the generalized eigenvalue equation:

$$HQ^q = E_q S Q^q \tag{25}$$

S is the overlap matrix in the atomic orbital basis, H is the Hamiltonian matrix which is determined from the extended Hückel theory (EHT) calculations. The extended Hückel

calculation is a semi-classical quantum chemistry method. Within the scheme of EHT, the off-diagonal Hamiltonian matrix can be given as follows:

$$H_{ij} = KS_{ij}\frac{H_{ii} + H_{jj}}{2} \tag{26}$$

where K is the Wolfsberg-Helmholtz constant, ~1.75. In EHT, only valence electrons are included; the core electron energies are assumed to be constant.

The population of the electron wave function can be determined from the overlap matrix and atomic orbital basis function,

$$P(t) = \left|\sum_{i,\alpha}^{MOL}\sum_{i,\beta} B^{*}_{i,\alpha}(t)B_{j,\beta}(t)S^{i,j}_{\alpha,\beta}\right| \tag{27}$$

The combination of theoretical methodology enables the realistic description of the ET process in the large system, and we have this method to investigate the ET in dye/TiO_2 interface. We have established the detailed mechanism of electron transfer in DSSC [40].

5. The titanium dioxide used as photocatalyst

Another important application of TiO_2 is a photocatalytic reaction. The titanium dioxide (TiO_2) has been also widely used as a photocatalyst. Numerous studies have been carried out on the popular photocatalysts of TiO_2. The reaction turns out to be very complicated, and its mechanism is still not well understood. It is time to use the theoretical tools to find some important insights out. Photoexcitation of TiO_2 leads to the formation of free electrons and holes in CB and VB, respectively. There are several carrier dynamic pathways that might happen. First, an electron in CB recombines non-radiatively with a hole in VB in the form of heat. Second, electron acceptors are reduced by photogenerated electrons; and third, electron donors are oxidized by photogenerated holes. The photochemical reaction may happen once the electron and hole diffuse to the TiO_2 crystal surface, and then the photogenerated electron and hole can interact with the O_2 or H_2O molecules to achieve the oxidization or reduction process. Some typical oxidization and reduction process are shown in **Figure 3**.

The elementary reaction steps can be expressed as follows:

$$\begin{aligned} &TiO_2 + hv(\lambda < 390nm) \rightarrow e^- + h^+ \\ &h^+ + H_2O \rightarrow OH^{\bullet} + H^+ \\ &e^- + O_2 \rightarrow O_2^- \end{aligned} \tag{28}$$

5.1. The surface of titanium dioxide

The performance of the TiO_2-based photocatalyst device can be regulated by the surface molecular adsorption, and particularly, the adsorption of O_2 and H_2O on TiO_2 has been widely discussed. Investigation of adsorption of H_2O onto TiO_2 mainly focuses on which sites water molecular adsorption is favored, and also the form of water adsorption, molecular or dissociative. Rutile

http://dx.doi.org/10.5772/intechopen.68745

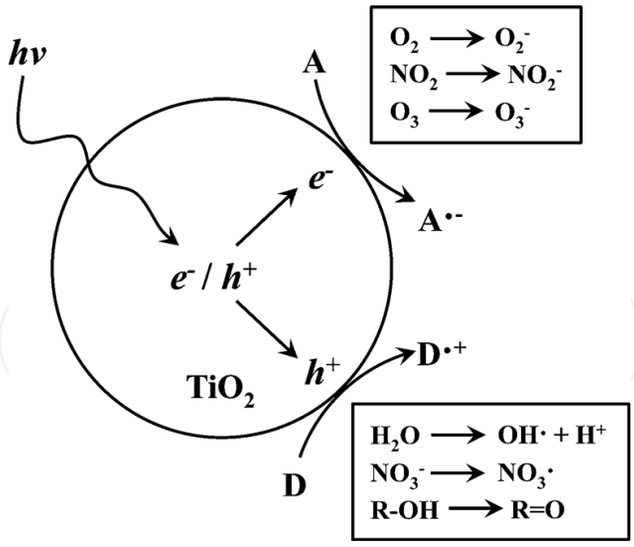

Figure 3. Schematic representation of typical photocatalyst process. (Copyright 2013 American Chemistry Society).

TiO_2 (110) surface, the most stable TiO_2 polymorph, is usually employed to model the surface adsorption. Experimentally, a water molecule was predicted on being molecularly adsorption onto the stoichiometric rutile TiO_2 (110) surface under the low coverage [41–44]. Theoretically, both molecularly and dissociative absorptions have been suggested by the DFT calculation [45–47]. The difference between theory and experiment arising from the exact parameters used in DFT calculation, such as the exchange-correlation function, and from the limitation in the simulation scales, for example, experimental system usually has the diameter up to tens of hundreds of angstrom, which is far beyond the capability DFT can handle at the current stage.

Band-gap engineering is an efficient way to tune the photoactive of the semiconductor. Different heteroatoms like anion nonmetals and cation-metals as well as cation-nonmetals have been used to doping in the semiconductor. Generally, semiconductor doping can introduce gap-state in the band gap, and this leads to the reduction of the optical band gap, improving the photoactive. Electronic structure calculation based on DFT has been used to elucidate the possible effect caused by the dopant. For example, substitute the Ti atom of bulk TiO_2 with metal cations, such as Cr and V, is an n-type doping. This will introduce the electron donor states within the band gap, which allows for the reduction of the optical band gap, thus the better performance for utilizing the photon energy, extending the photocatalytic activity into visible part of the solar spectrum [48–51]. Replace the O with N or C atoms belongs to the p-doping, which introduce the electron acceptor states. Therefore, dopant states have the large extent of overlap between the electronic states of TiO_2, this minimizing the problems arising with the localized states in n-type doping.

5.2. The CO_2 photocatalytic reaction

From the viewpoints of a theoretical worker, one can determine the every property of a given materials using just its coordinates, and this is exactly the idea of first-principles calculation.

The properties include the geometrical structure, the ground state energy, the work function, and the band structure. In order to design the more efficient photocatalyst, it is necessary for theoretical worker knows the basic physics prior to performing first principle calculations.

First, the photocatalyst performance depends on the chosen of the TiO_2 surface. Asymmetric anatase (101) surface has the most uncoordinated Ti and O atoms, and thus, it is suitable for the molecular adsorption of CO_2, thus the better photocatalyst performance (**Figure 4**). Second, proper energy alignment between TiO_2 and the adsorbed molecules is required. This is due to the built-in driving force largely affect the direction of the ET, and a negative driving force should lead to the inefficient ET process, in order to avoid this issue. The TiO_2 CB should be higher than the molecular LUMO orbital, whereas the TiO_2 VB should be lower than the molecular HOMO orbital. Third, the interface details between TiO_2 and adsorbed molecule affect the time scale of interface charge separation. This is because interface charge transfer can be described using the Fermi's Golden rule if the coupling between the electron/hole donor orbital in TiO_2 and acceptor orbital in adsorbed molecule is large, then the ET will be fast. The interface interaction depends on the adsorption details of molecular onto TiO_2 surfaces.

The last, the work function is defined as the minimum energy required transferring an electron from the highest filled level of a solid to a point in the vacuum outside the solid surface. The work function is a property of the surface, which has been widely used to measure how difficult the charge transfer is. Screen the materials with the proper work function is required.

5.3. Other main photocatalytic reactions

The (101)-(001) surface heterojunction constructed on polyhedral TiO_2 nanocrystals has recently been proposed to be favorable for the efficient electron-hole spatial separation due

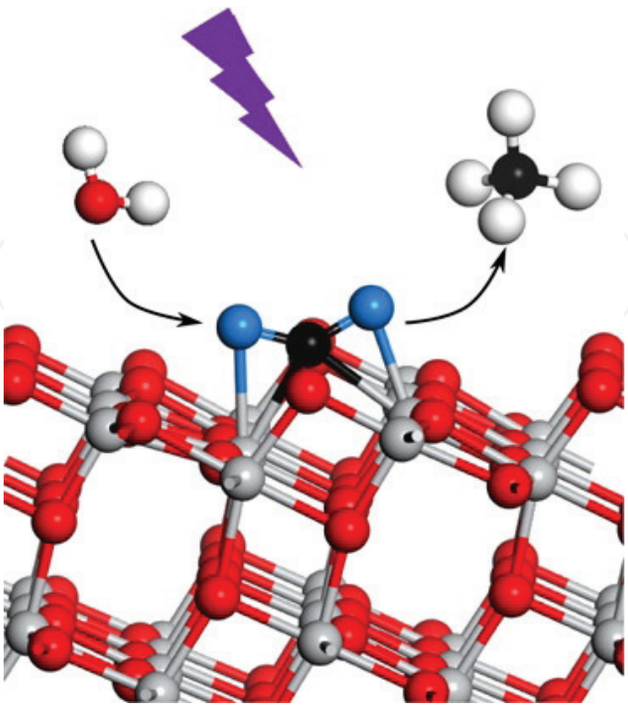

Figure 4. Photocatalytic reduction of CO_2 on the anatase TiO_2 (101) surface (Copyright 2016 American Chemical Society).

to the preferential accumulation of electron and hole on (101) and (001) facets, respectively. The formed free electron and hole can promote reactive oxygen species (ROS) production, which potentially can be used for inactivation of bacteria. For the biological system, the theoretical investigation with electronic level is still a challenging for researchers and here only an example for readers a general understanding. A series of truncated octahedral double cone TiO_2 nanocrystals co-planar with (101) and (001) facets are prepared to form (101) to (100) of various ratios for optimizing the electron-(001) surface. All of these polyhedral TiO_2 nanocrystals can produce ROS more prominently than spherical TiO_2 nanocrystals, exhibiting more bacteria against gram-negative (E. coli) and Gram-positive (*Staphylococcus aureus*) bacteria under simulated sunlight high antibacterial activity. Surface heterojunction as a new strategy is expected to develop effective antimicrobial nanomaterials [52].

6. Summary

In this chapter, we aimed to review and summarize of recent important theoretical studies of titanium dioxide for dye-sensitized solar cell and photocatalytic reaction. How to build a suitable TiO_2 model to start a theoretical study for fast interfacial electron transfer between the dye and TiO_2 in DSSC system, and the mechanism for photocatalytic reactions on the TiO_2 surface will be impressive for readers. We need to describe the electronic band structure of excited state or ground state of TiO_2, the surface morphology, active energy for reaction as well as the fast interfacial electron transfer between the adsorbed molecule and TiO_2 accurately for fine theoretical studies. For some situation, we also need to do molecular dynamics for the surface structure of adsorbed TiO_2. May the summary report will help the readership to strengthen the fundamental knowledge or to find more interesting ideas.

Acknowledgements

The authors thank Jilin University and Young Scholar Training Program of Jilin University. The authors gratefully acknowledge support from the National Natural Science Foundation of China (Grant No. 21573088).

Author details

Fu-Quan Bai*, Wei Li and Hong-Xing Zhang

*Address all correspondence to: baifq@jlu.edu.cn

International Joint Research Laboratory of Nano-Micro Architecture Chemistry, Institute of Theoretical Chemistry, Jilin University, Changchun, China

References

[1] Gratzel M. Recent advances in sensitized mesoscopic solar cells. Accounts of Chemical Research. 2009;**42**(11):1788-1798. DOI: 10.1021/ar900141y

[2] Hu S, Majumdar A. Opportunities and challenges for a sustainable energy future. Nature. 2012;**488**(7411):294–303. DOI: 10.1038/nature11475

[3] Kojima A, Teshima K, Shirai Y, Miyasaka T. Organometal halide perovskites as visible-light sensitizers for photovoltaic cells. Journal of the American Chemical Society. 2009;**131** (17):6050-6051. DOI: 10.1021/ja809598r

[4] Desilvestro J, Grätzel M, Kavan L, Moser J, Augustynski J. Highly efficient sensitization of titanium dioxide. Journal of the American Chemical Society. 1985;**107**(10):2988–2990

[5] Lee MM, Teuscher J, Miyasaka T, Murakami TN, Snaith HJ. Efficient hybrid solar cells based on meso-superstructured organometal halide perovskites. Science. 2012;**338**(6107):643–647. DOI: 10.1126/science.1228604

[6] Liu D, Kelly TL. Perovskite solar cells with a planar heterojunction structure prepared using room-temperature solution processing techniques. Nature Photonics. 2014;**8**:133–138. DOI: 10.1038/nphoton.2013.342

[7] Snaith HJ, Schmidt-Mende L. Advances in liquid-electrolyte and solid-state dye-sensitized solar cells. Advanced Materials. 2007;**19**(20):3187–3200. DOI: 10.1002/adma.200602903

[8] Souza C, Tosoni, Illas F. Theoretical approaches to excited-state-related phenomena in oxide surfaces. Chemical Reviews. 2013;**113**:4456–4495. DOI: 10.1021/cr300228z

[9] Pelaez M, Nolan NT, Pillai SC, Seery MK, Falaras P, Kontos AG, Dunlop PSM, Hamilton JWJ, Byrne JA, O'Shea K, Entezari MH, Dionysiou DD. A review on the visible light active titanium dioxide photocatalysts for environmental applications. Applied Catalysis B: Environmental. 2012;**125**:331-349. DOI: 10.1016/j.apcatb.2012.05.036

[10] Na-Phattalung S, Smith MF, Kim K, Du MH, Wei SH, Zhang SB, Limpijumnong S. First-principles study of native defects in anatase TiO_2. Physical Review B: Condensed Matter and Materials Physics. 2006;**73**:125205. DOI: 10.1103/PhysRevB.73.125205

[11] Mehta P, Salvador PA, Kitchin JR. Identifying potential BO2 oxide polymorphs for epitaxial growth candidates. ACS Applied Materials Interfaces. 2014;**6**(5):3630–3639. DOI: 10.1021/am4059149

[12] Curnan MT, Kitchin JR. Investigating the energetic ordering of stable and metastable TiO_2 polymorphs using DFT+U and hybrid functionals. Journal of Physical Chemistry C. 2015;**119**(36):21060–21071. DOI: 10.1021/acs.jpcc.5b05338

[13] Dompablo MEA, Morales-Garcıa A, Taravillo M.: DFT+U calculations of crystal lattice, electronic structure, and phase stability under pressure of TiO_2 polymorphs. Journal of Chemical Physics. 2011;**135**:054503. DOI: 10.1063/1.3617244

[14] Vu NH, Le HV, Cao TM, Pham VV, Le HM, Nguyen-Manh D. Anatase–rutile phase transformation of titanium dioxide bulk material: A DFT + U approach. Journal of Physics: Condensed Matter. 2012;**24**:405501. DOI: 10.1088/0953-8984/24/40/405501

[15] Casadei M, Ren X, Rinke P, Rubio A, Scheffler M. Density-functional theory for f-electron systems: The $\alpha-\gamma$ phase transition in cerium. Physical Review Letters. 2012;**109**(14):146402. DOI: 10.1103/PhysRevLett.109.146402

[16] Peng H, Lany S. Polymorphic energy ordering of MgO, ZnO, GaN, and MnO within the random phase approximation. Physical Review B. 2013;**87**(17):174113. DOI: 10.1103/PhysRevB.87.174113

[17] Cui ZH, Wu F, Jiang H. First-principles study of relative stability of rutile and anatase TiO_2 using the random phase approximation. Physical Chemistry Chemical Physics. 2016;**18**(43):29914–29922. DOI: 10.1039/C6CP04973G

[18] Runge E, Gross EKU. Density-functional theory for time-dependent systems. Physical Review Letters. 1984;**52**(12):997. DOI: 10.1103/PhysRevLett.52.997

[19] Hirata S, Head-Gordon M, Bartlett RJ. Configuration interaction singles, time-dependent Hartree–Fock, and time-dependent density functional theory for the electronic excited states of extended systems. The Journal of Chemical Physics. 1999;**111**(24):10774–10786. DOI: 10.1063/1.480443

[20] Izmaylov AF, Scuseria GE. Why are time-dependent density functional theory excitations in solids equal to band structure energy gaps for semilocal functionals, and how does nonlocal Hartree–Fock-type exchange introduce excitonic effects?. The Journal of chemical physics. 2008;**129**(3):034101. DOI: 10.1063/1.2953701

[21] Bernasconi L, Tomić S, Ferrero M, Rerat M, Orlando R, Dovesi R, Harrison NM. First-principles optical response of semiconductors and oxide materials. Physical Review B. 2011;**83**(19):195325. DOI: 10.1103/PhysRevB.83.195325

[22] Walker B, Saitta AM, Gebauer R, Baroni S. Efficient approach to time-dependent density-functional perturbation theory for optical spectroscopy. Physical Review Letters. 2006;**96**(11):113001. DOI: 10.1103/PhysRevLett.96.113001

[23] Anisimov VI, Aryasetiawan F, Lichtenstein AI. First-principles calculations of the electronic structure and spectra of strongly correlated systems: The LDA+ U method. Journal of Physics: Condensed Matter. 1997;**9**(4):767. DOI: 0953-8984/9/4/002

[24] Hedin L. New method for calculating the One-Particle Green's function with application to the Electron-Gas problem. Physical Review. 1965;**139**:A796. DOI: 10.1103/PhysRev.139.A796

[25] Huang P, Carter EA. Advances in correlated electronic structure methods for solids, surfaces, and nanostructures. Annual Review of Physical Chemistry. 2008;**59**:261–290. DOI: 10.1146/annurev.physchem.59.032607.093528

[26] Onida G, Reining L, Rubio A. Electronic excitations: density-functional versus many-body Green's-function approaches. Reviews of Modern Physics. 2002;**74**(2):601. DOI: 10.1103/RevModPhys.74.601

[27] Matsui M, Akaogi M. Molecular dynamics simulation of the structural and physical properties of the four polymorphs of TiO_2. Molecular Simulation. 1991;**6**(4–6):239–244. DOI: 10.1080/08927029108022432

[28] Swamy V, Gale JD. Transferable variable-charge interatomic potential for atomistic simulation of titanium oxides. Physical Review B. 2000;**62**(9):5406. DOI: 10.1103/PhysRevB.62.5406

[29] Koparde VN, Cummings PT. Molecular dynamics study of water adsorption on TiO_2 nanoparticles. The Journal of Physical Chemistry C. 2007;**111**(19):6920–6926. DOI: 10.1021/jp0666380

[30] Selcuk S, Selloni A. Facet-dependent trapping and dynamics of excess electrons at anatase TiO_2 surfaces and aqueous interfaces. Nature Materials. 2016;**15**(10):1107–1112. DOI: 10.1038/nmat4672

[31] Vittadini A, Selloni A, Rotzinger FP, Grätzel, M. Formic acid adsorption on dry and hydrated TiO_2 anatase (101) surfaces by DFT calculations. The Journal of Physical Chemistry B. 2000;**104**(6):1300–1306. DOI: 10.1021/jp993583b

[32] Grätzel M. Perspectives for dye-sensitized nanocrystalline solar cells. Progress in Photovoltaics: Research and Applications. 2000;**8**(1):171–185. DOI: 10.1002/(SICI)1099-159X

[33] Akimov AV, Neukirch AJ, Prezhdo OV. Theoretical insights into photoinduced charge transfer and catalysis at oxide interfaces. Chemical Reviews. 2013;**113**(6):4496–4565. DOI: 10.1021/cr3004899

[34] Pan D, Klymyshyn N, Hu D. Tip-enhanced near-field Raman spectroscopy probing single dye-sensitized TiO_2 nanoparticles. Applied Physics Letters. 2006;**88**(9):093121. DOI: 10.1063/1.2176865

[35] Marcus RA.: Interaction of theory and experiment: examples from single molecule studies of nanoparticles. Philosophical Transactions of the Royal Society of London A: Mathematical, Physical and Engineering Sciences. 2010;**368**(1914):1109–1124. DOI: 10.1098/rsta.2009.0261

[36] Labat F, Ciofini I, Hratchian HP, Frisch M, Raghavachari K, Adamo C. First principles modeling of eosin-loaded ZnO films: A step toward the understanding of dye-sensitized solar cell performances. Journal of the American Chemical Society. 2009;**131**(40):14290–14298. DOI 10.1021/ja902833s

[37] Persson P, Lundqvist M J, Ernstorfer R, Goddard WA, Willig F. Quantum chemical calculations of the influence of anchor-cum-spacer groups on femtosecond electron transfer times in dye-sensitized semiconductor nanocrystals. Journal of Chemical Theory and Computation. 2006;**2**(2):441–451. DOI: 10.1021/ct050141x

[38] Tully JC. Molecular dynamics with electronic transitions. The Journal of Chemical Physics. 1990;**93**(2):1061–1071. DOI: 10.1063/1.459170

[39] Herman MF. Nonadiabatic semiclassical scattering. I. Analysis of generalized surface hopping procedures. The Journal of Chemical Physics. 1984;**81**(2):754–763. DOI: 10.1063/1.447708

[40] Li W, Rego LGC, Bai FQ. What makes hydroxamate a promising anchoring group in dye-sensitized solar cells? onsights from theoretical investigation. The Journal of Physical Chemistry Letters. 2014;**5**(22):3992–3999. DOI: 10.1021/jz501973d

[41] Kurtz RL, Stock-Bauer R, Msdey TE. Synchrotron radiation studies of H_2O adsorption on TiO_2 (110). Surface Science. 1989;**218**(1):178–200. DOI: 10.1016/0039-6028(89)90626-2

[42] Hugenschmidt MB, Gamble L, Campbell CT. The interaction of H_2O with a TiO_2 (110) surface. Surface Science. 1994;**302**(3):329–340. DOI: 10.1016/0039-6028(94)90837-0

[43] Henderson MA. An HREELS and TPD study of water on TiO_2 (110): The extent of molecular versus dissociative adsorption. Surface Science. 1996;**355**(1–3):151–166. DOI: 10.1016/0039-6028(95)01357-1

[44] Epling WS, Peden CHF, Henderson MA. Evidence for oxygen adatoms on TiO_2 (110) resulting from O_2 dissociation at vacancy sites. Surface Science. 1998;**412**:333–343. DOI: 10.1016/S0039-6028(98)00446-4

[45] Lindan PJD, Harrison NM, Gillan MJ. Mixed dissociative and molecular adsorption of water on the rutile (110) surface. Physical Review Letters. 1998;**80**(4):762. DOI: 10.1103/PhysRevLett.80.762

[46] Harris LA, Quong AA. Molecular chemisorption as the theoretically preferred pathway for water adsorption on ideal rutile TiO_2 (110). Physical Review Letters. 2004;**93**(8):086105. DOI: 10.1103/PhysRevLett.93.086105

[47] Zhang C, Lindan PJD. A density functional theory study of the coadsorption of water and oxygen on TiO_2 (110). The Journal of Chemical Physics. 2004;**121**(8):3811–3815. DOI: 10.1063/1.1775784

[48] Wang F, Di Valentin C, Pacchioni G. Doping of WO_3 for photocatalytic water splitting: Hints from density functional theory. The Journal of Physical Chemistry C. 2012;**116**(16):8901–8909. DOI: 10.1021/jp300867j

[49] Asahi R, Morikawa T, Ohwaki T. Visible-light photocatalysis in nitrogen-doped titanium oxides. Science. 200;**293**(5528):269–271. DOI: 10.1126/science.1061051

[50] Borgarello E, Kiwi J, Gratzel M. Visible light induced water cleavage in colloidal solutions of chromium-doped titanium dioxide particles. Journal of the American Chemical Society. 1982;**104**(11):2996–3002. DOI: 10.1021/ja00375a010

[51] Li M, Zhang J, Guo D. Band gap engineering of compensated (N, H) and (C, 2H) codoped anatase TiO_2: A first-principles calculation. Chemical Physics Letters. 2012;**539**:175–179. DOI: 10.1016/j.cplett.2012.04.057

[52] Liu N, Chang Y, Feng YL, Cheng Y, Sun XJ, Jian H, Feng YQ, Xi Li, Zhang HY. {101}-{001} Surface heterojunction-enhanced antibacterial activity of titanium dioxide nanocrystals under sunlight irradiation. ACS Applied Materials & Interfaces. 2017;**9**(7):5907–5915. DOI: 10.1021/acsami.6b16373